

Stochastic Axion Dark Matter in Axion Landscape

Shota Nakagawa[♣] Fuminobu Takahashi^{♣◇} Wen Yin[♡]

[♣] Department of Physics, Tohoku University, Sendai, Miyagi 980-8578, Japan

[◇] Kavli IPMU (WPI), UTIAS, The University of Tokyo, Kashiwa, Chiba 277-8583, Japan

[♡] Department of Physics, Korea Advanced Institute of Science and Technology, Daejeon 34141, Korea

Abstract. We study the stochastic axion dark matter scenario in the axion landscape, where one of the axions is light and stable and therefore explains dark matter. If the axion mass at the potential is a typical value of the curvature along the direction, the potential can be well approximated by a quadratic mass term. On the other hand, if the axion mass happens to be suppressed in the vicinity of the minimum, the potential may be approximated by a quartic potential plus a suppressed quadratic one, for which the initial angle, and thus the axion abundance, can be significantly suppressed compared to the quadratic case. We delineate the viable parameter region by taking account of various observational constraints, and find that a broader range of the inflation scale is allowed. Also, if the curvature of the potential is suppressed over a certain range of the potential, the onset of coherent oscillations can be delayed. Then, the axion dark matter with a small decay constant is possible. We also discuss the π inflation mechanism to realize the hilltop initial condition in the stochastic axion scenario.

Contents

1	Introduction	1
2	Light axion in the axion landscape	2
3	Bunch-Davies distribution and axion abundance	4
3.1	Bunch-Davies distribution	5
3.2	Axion abundance	7
3.2.1	The case of the quadratic potential	9
3.2.2	The case of the quartic potential	10
3.2.3	Thermal axion particle production	11
4	Cosmological bounds	12
4.1	Isocurvature perturbations	13
4.1.1	The case of the quadratic potential	13
4.1.2	The case of the quartic potential	13
4.2	Axion decay into photons and hidden photons	14
4.3	Primordial tensor mode	16
4.4	Results	16
5	Delayed onset of oscillations and πinflation	19
6	Conclusions	21

1 Introduction

The identity of dark matter remains a great mystery. Dark matter is known to be very stable, and its lifetime must be much longer than the present age of the universe [1]. The stability of dark matter can be explained in various ways, and one plausible possibility is that it is due to the small mass and feeble interactions with the standard model particles.

In the string theory, a large number of moduli or axions appear in the low-energy effective theory after compactifying the extra dimensions. Some of them may remain so light that they play an important role in cosmology such as the inflaton, dark energy, or dark matter. Indeed, an axion is known to be a plausible candidate for dark matter; it is stable on cosmological time scales due to its small mass and feeble interactions, and moreover, it can be copiously produced by the vacuum misalignment mechanism [2–4]. In this paper we study the string axion (simply axion hereafter) as a dark matter candidate.

The axion abundance depends on the initial misalignment angle and the global shape of the potential. Usually one adopts the initial angle θ_{ini} of order unity to estimate the axion abundance. Recently, however, it was pointed out in Refs. [5, 6] (including two of the present authors F.T. and W.Y.) that the typical value of θ_{ini} can be naturally much smaller than unity if the inflation scale is low and if the inflation lasts sufficiently long. This is because the stochastic behavior of the axion is balanced by the classical dynamics after sufficiently long inflation, and its probability distribution reaches equilibrium, the so-called Bunch-Davies (BD) distribution [7] peaked at the potential minimum. In some sense, the axion knows

where the minimum is in a probabilistic way. The BD distribution was applied to the string axion in Ref. [8], in which it was shown that the moduli problem induced by the string axion can be significantly alleviated.

The other important factor of the axion abundance is the shape of the axion potential. If there are many axions with mass and kinetic mixings, they may form a complicated axion landscape [9, 10], which has interesting implications for inflation models [9–14] and dark matter [15]. In order for one of the axions to explain dark matter, its mass must be extremely light compared to the fundamental scale. Broadly speaking, such a light axion mass can be realized in the following two cases: (i) there is a flat direction in the axion landscape, along which the axion potential is extremely flat; (ii) the axion mass is suppressed in the vicinity of a potential minimum due to cancellation among different contributions. In the first case, the potential is well approximated by a quadratic term when expanded around the minimum, and the axion abundance in this case is the one usually adopted in the literature. In the second case, on the other hand, the light axion mass is just a consequence of cancellation, and it implies that the quartic coupling is not generally suppressed. Therefore, it is likely that the potential can be approximated by a quartic potential plus a tiny mass term when expanded around the minimum. The cancellation may be due to the anthropic requirement for dark matter. In Ref. [15] the axion abundance and its isocurvature fluctuations were studied in a set-up corresponding to the second case. It was assumed that the initial misalignment angle was such that the curvature of the potential becomes comparable to the Hubble parameter during inflation. However, it was not studied how the viable parameter region will be modified if one uses the BD distribution as the initial condition. The suppressed initial angle has two effects. One is to suppress the axion abundance. The other is to enhance the isocurvature perturbation for a fixed inflation scale. The purpose of this paper is to study these effects in detail and show the viable parameter space in this scenario.

In this paper we study the stochastic axion scenario where the initial misalignment angle follows the probability distribution determined by the competition between the quantum diffusion and the classical motion. We allow the axion potential to deviate from a simple quadratic potential, and estimate the axion abundance and isocurvature perturbations to delineate the viable parameter space. We will take account of various cosmological bounds such as non-detection of the primordial gravitational waves and the upper bound on the extra diffuse X-ray/ γ -ray fluxes. As we shall see, a broader range of the inflation scale is allowed in the case where the axion potential is approximated by the quartic plus tiny quadratic terms compared to the conventional case with the simple mass term.

The rest of this paper is organized as follows. In Sec. 2 we explain the set-up for the axion potential. After a brief review of the stochastic axion scenario, we estimate the initial misalignment angle and the resultant axion abundance in Sec. 3. In Sec. 4 various cosmological bounds are taken into account to delineate the viable parameter space. The last two sections are devoted to discussion and conclusions.

2 Light axion in the axion landscape

Let us suppose that there are many axions which have mass and kinetic mixings and constitute a complex landscape, the so-called axion landscape [9, 10]. The axion potential can be

modeled by

$$V(\phi_\alpha) = \sum_{i=1}^{N_s} \Lambda_i^4 \left(1 - \cos \left(\sum_{\alpha=1}^{N_A} n_{i\alpha} \frac{\phi_\alpha}{f_\alpha} + \delta_i \right) \right) + C, \quad (2.1)$$

where the prefactor Λ_i and δ_i respectively represent the dynamical scale and a CP phase of the corresponding non-perturbative effect, $n_{i\alpha}$ is an integer-valued anomaly coefficient matrix, f_α is the decay constant, and N_s and N_A are the number of shift symmetry breaking terms and axions, respectively. The constant term C is chosen so that the cosmological constant is vanishingly small in the present universe. In this paper we assume that one of the axions is responsible for the observed dark matter. To this end, the axion must be sufficiently long-lived, implying that its mass is very light. Broadly speaking, there are two possibilities to realize such a light axion in the axion landscape. One possibility is that there exists a flat direction in the landscape. It may be that the corresponding dynamical scale happens to be much smaller than the other directions, or the effective decay constant may be enhanced by the KNP mechanism [10, 16, 17]. Although the enhanced decay constant certainly makes the axion lighter, we consider the former case because the axion mass must be extremely light to have a lifetime longer than the present age of the universe, and the latter would require a rather contrived set-up to realize such a large hierarchy in the effective decay constants. Focusing on the flat direction, we consider the potential modeled by a single cosine term,

$$V(\phi) = \Lambda^4 \left[1 - \cos \left(\frac{\phi}{f_\phi} \right) \right] \simeq \frac{1}{2} m_\phi^2 \phi^2, \quad (2.2)$$

where Λ denotes the potential height, f_ϕ is the axion decay constant, and we have expanded the potential at the origin in the second equality for $|\phi| \lesssim f_\phi$. The axion mass m_ϕ is given by

$$m_\phi = \frac{\Lambda^2}{f_\phi}, \quad (2.3)$$

and we assume $\Lambda \ll f_\phi$.

The other possibility is that the axion mass at one of the potential minima in the landscape happens to be much smaller than the typical curvature scale. This can be realized by cancellation among several shift symmetry breaking terms. For example, a single axion with two shift symmetry breakings satisfying this property was considered in Ref. [15], and its potential is given by

$$V(\phi) = \Lambda_1^4 \left[1 - \cos \left(n_1 \frac{\phi}{f_\phi} \right) \right] + \Lambda_2^4 \left[1 - \cos \left(n_2 \frac{\phi}{f_\phi} + \delta \right) \right] + \text{const.}, \quad (2.4)$$

where Λ_1 and Λ_2 represent the size of the shift symmetry breakings, and δ is the CP phase between the two terms. The axion mass can be suppressed if the contributions of the two terms are almost canceled at the minimum. Specifically we consider $\delta = \pi$ and $n_2 > n_1$, and expand the potential around the minimum at $\phi = 0$ as

$$V(\phi) \simeq \frac{1}{2} m_\phi^2 \phi^2 + \frac{\lambda}{4!} \phi^4 \quad (2.5)$$

for $|\phi| < f_\phi$. Here, the axion mass m_ϕ and the quartic coupling λ are respectively given by

$$m_\phi^2 = \frac{n_1^2 \Lambda_1^4 - n_2^2 \Lambda_2^4}{f_\phi^2}, \quad (2.6)$$

$$\lambda = \frac{n_2^4 \Lambda_2^4 - n_1^4 \Lambda_1^4}{f_\phi^4} \simeq (n_2^2 - n_1^2) \frac{n_1^2 \Lambda_1^4}{f_\phi^4}, \quad (2.7)$$

where in the last equality, we have used the fact that the two shift symmetry breaking terms are almost canceled to realize the light axion mass, i.e.,

$$\frac{n_1^2 \Lambda_1^4}{f_\phi^2} \simeq \frac{n_2^2 \Lambda_2^4}{f_\phi^2} \gg m_\phi^2.$$

On the other hand, the quartic coupling and higher order terms are not suppressed in general. To be concrete, we will set $n_1 = 1$ and $n_2 = 2$ in which case the periodicity of the potential is equal to $2\pi f_\phi$.

For later use we also define a dimensionless angle,

$$\theta \equiv \frac{\phi}{f_\phi}.$$

The axion potential changes from the quadratic to quartic term around $\theta \simeq \theta_{\text{tr}}$ defined by

$$\theta_{\text{tr}} \equiv \frac{m_\phi}{f_\phi} \sqrt{\frac{6}{\lambda}} \simeq \sqrt{\frac{6}{n_2^2 - n_1^2}} \frac{f_\phi m_\phi}{\Lambda_1^2} \ll 1. \quad (2.8)$$

Precisely speaking, we define θ_{tr} such that the derivative of the quadratic term becomes equal to that of the quartic term at $\theta = \theta_{\text{tr}}$, since we are interested in the transition of the axion oscillations whose periodicity depends on $V'(\phi)$ at the oscillation amplitude.

3 Bunch-Davies distribution and axion abundance

If the axion is light during inflation, it acquires quantum fluctuations of order the Hubble parameter, H_{inf} . The fluctuations continuously exit the horizon and become classical soon afterwards. Those fluctuations can be treated as a random Gaussian noise. Therefore, while the axion is classically driven toward the potential minimum, it is also randomly kicked upward or downward on the potential by the small-scale fluctuations. Such stochastic axion dynamics can be well described by the Fokker-Planck equation that takes account of the effect of the random Gaussian noise as a diffusion effect on the axion probability distribution. Then, the two competing effects end up with an equilibrium distribution of the axion field, if inflation lasts long enough. This probability distribution is called the BD distribution [7]. It was shown in Refs. [5, 6] that the QCD axion abundance can be suppressed if the initial angle follows the BD distribution.

In the following we derive the BD distribution of the initial angle θ_{ini} as a function of the inflation scale for a general axion potential. Then, we estimate the axion abundance by applying it to the quadratic or quartic potentials.

3.1 Bunch-Davies distribution

We assume that the Hubble parameter during inflation, H_{inf} , is approximately constant in time, and derive the BD distribution for the axion field, ϕ . First, let us separate it into the long and short wave-length modes, $\phi = \bar{\phi} + \delta\phi_{\text{short}}$. The axion dynamics under the effect of short-wavelength fluctuations is described by the Langevin equation,

$$\dot{\bar{\phi}} = -\frac{1}{3H_{\text{inf}}}V'(\bar{\phi}) + f(\mathbf{x}, t), \quad (3.1)$$

where $V(\phi)$ is a periodic potential of ϕ and the dot and prime represent the derivative with respect to the cosmic time t and axion field ϕ , respectively. We assume that $V(\phi)$ is negligibly small compared to the total energy density of the universe, and it satisfies $|V''(\phi)| \ll H_{\text{inf}}^2$ for all values of ϕ so that the stochastic formalism is applicable. The information of the short wave-length mode $\delta\phi_{\text{short}}$ is included in the Gaussian noise term, $f(\mathbf{x}, t)$, satisfying

$$\langle f(\mathbf{x}, t_1)f(\mathbf{x}, t_2) \rangle = \frac{H_{\text{inf}}^3}{4\pi^2}\delta(t_1 - t_2), \quad (3.2)$$

where $\langle \dots \rangle$ represents the stochastic average. The corresponding Fokker-Planck equation is given by

$$\frac{\partial \mathcal{P}(\phi, t)}{\partial t} = \frac{1}{3H_{\text{inf}}}\frac{\partial}{\partial \phi}(V'(\phi)\mathcal{P}(\phi, t)) + \frac{H_{\text{inf}}^3}{8\pi^2}\frac{\partial^2 \mathcal{P}(\phi, t)}{\partial \phi^2}, \quad (3.3)$$

where $\mathcal{P}(\phi, t)$ denotes the probability distribution for the coarse-grained field ϕ .

We are interested in the asymptotic form of the probability distribution, $\mathcal{P}_{\text{BD}}(\phi)$, which satisfies

$$\frac{1}{3H_{\text{inf}}}V'(\phi)\mathcal{P}_{\text{BD}}(\phi) + \frac{H_{\text{inf}}^3}{8\pi^2}\frac{\partial \mathcal{P}_{\text{BD}}(\phi)}{\partial \phi} = 0. \quad (3.4)$$

This equation follows from the Fokker-Planck equation with $\partial \mathcal{P}(\phi, t)/\partial t = 0$ under the assumption that $V(\phi)$ and $\mathcal{P}_{\text{BD}}(\phi)$ are periodic with respect to ϕ .¹ The solution is given by

$$\mathcal{P}_{\text{BD}}(\phi) \propto \exp\left(-\frac{8\pi^2}{3H_{\text{inf}}^4}V(\phi)\right). \quad (3.5)$$

This is called the BD distribution. Therefore, the BD distribution is the largest where $V(\phi)$ is the smallest.

For convenience, we define the probability distribution for the dimensionless angle $\theta = \phi/f_\phi$ as

$$P(\theta) \propto \mathcal{P}_{\text{BD}}(\theta f_\phi). \quad (3.6)$$

In the following we set the origin of θ equal to one of the minima of $V(\phi)$, and consider the probability distribution around it in the range of $\theta_- \leq \theta \leq \theta_+$. The boundary is given by $\theta_\pm = \pm\pi$ for the two potentials given in the previous section. The proportionality factor is determined by the normalization condition,

$$\int_{\theta_-}^{\theta_+} P(\theta)d\theta = 1, \quad (3.7)$$

¹Alternatively, one may assume that the probability distribution vanishes at the boundary of ϕ .

where we implicitly assume that $P(\theta)$ is vanishingly small at the boundary. We will comment on the case where this is not satisfied at the end of this subsection. Using the above probability distribution, we can define the typical initial angle as the variance,

$$\theta_{\text{ini}} \equiv \sqrt{\langle \theta^2 \rangle} = \left(\int_{\theta_-}^{\theta_+} \theta^2 P(\theta) d\theta \right)^{1/2}. \quad (3.8)$$

In the case of the quadratic potential (2.2), the probability distribution is given by the Gaussian form,

$$P(\theta) \propto \exp \left[-\frac{4\pi^2 m_\phi^2 f_\phi^2}{3H_{\text{inf}}^4} \theta^2 \right] \quad (|\theta| \lesssim 1), \quad (3.9)$$

where one can see that the distribution is peaked at the potential minimum $\theta = 0$, and it is unlikely for θ to take values much greater than $H_{\text{inf}}^2/m_\phi f_\phi$. Using (3.8) and (3.9), one can estimate the initial angle θ_{ini} as

$$\theta_{\text{ini}} \simeq 1.9 \times 10^{-6} \left(\frac{H_{\text{inf}}}{10^5 \text{ GeV}} \right)^2 \left(\frac{f_\phi}{10^{16} \text{ GeV}} \right)^{-1} \left(\frac{m_\phi}{100 \text{ MeV}} \right)^{-1}, \quad (3.10)$$

which can be naturally much smaller than unity without fine-tuning the initial condition. Note that this expression is valid only for $\theta_{\text{ini}} \lesssim 1$.

Similarly, in the case of the potential given by (2.5), the probability distribution is approximately given by

$$P(\theta) \propto \begin{cases} \exp \left[-\frac{\lambda \pi^2 f_\phi^4}{9H_{\text{inf}}^4} \theta^4 \right] & (\theta_{\text{tr}} \lesssim |\theta| \lesssim 1) \\ \exp \left[-\frac{4\pi^2 m_\phi^2 f_\phi^2}{3H_{\text{inf}}^4} \theta^2 \right] & (|\theta| \lesssim \theta_{\text{tr}}) \end{cases}. \quad (3.11)$$

Using (3.8) and (3.11), one can estimate the initial angle θ_{ini} as

$$\theta_{\text{ini}} \simeq \begin{cases} 4.3 \times 10^{-5} \left(\frac{H_{\text{inf}}}{10^8 \text{ GeV}} \right) \left(\frac{\Lambda_1}{10^{12} \text{ GeV}} \right)^{-1} & (\theta_{\text{tr}} \lesssim \theta_{\text{ini}} \lesssim 1) \quad (3.12) \\ 1.9 \times 10^{-6} \left(\frac{H_{\text{inf}}}{10^5 \text{ GeV}} \right)^2 \left(\frac{f_\phi}{10^{16} \text{ GeV}} \right)^{-1} \left(\frac{m_\phi}{100 \text{ MeV}} \right)^{-1} & (\theta_{\text{ini}} \lesssim \theta_{\text{tr}}). \quad (3.13) \end{cases}$$

We show the probability distribution $P(\theta)$ in Fig. 1 for several values of H_{inf} . This is the case that the axion populates the approximated potential (2.5) with $f_\phi = 10^{16} \text{ GeV}$, $\lambda = 3 \times 10^{-16}$, and $m_\phi = 1 \text{ eV}$. One can see that the distribution gets broader as H_{inf} increases. This is because the diffusion effect is stronger for larger H_{inf} . In other words, the initial angle is sharply peaked at the potential minimum for a sufficiently small H_{inf} .

In Fig. 2 we show θ_{ini} as a function of H_{inf} for $\Lambda_1 = 10^{12} \text{ GeV}$, $m_\phi = 1 \text{ eV}$, and $f_\phi = 10^{16} \text{ GeV}$. Here we substitute the original potential (2.4) into (3.8) to calculate θ_{ini} numerically. The dotted horizontal line shows the transition point from quadratic to quartic potential, $\theta_{\text{ini}} = \theta_{\text{tr}}$. One can see that θ_{ini} tends to be suppressed when the potential is

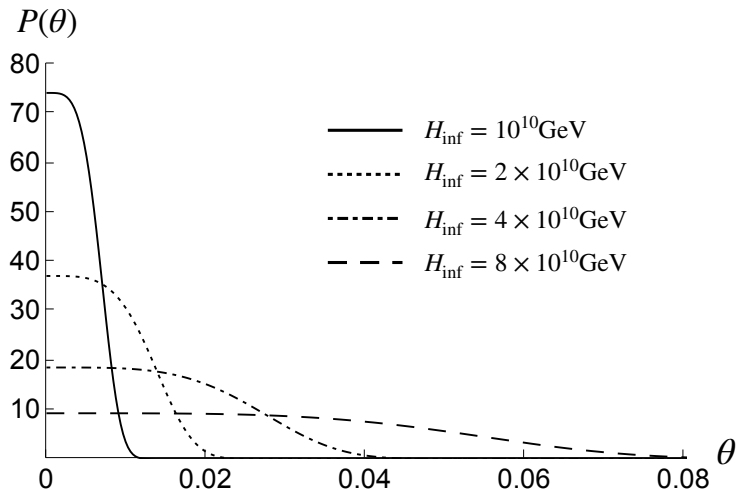


Figure 1. The BD distribution as a function of θ for several values of H_{inf} in the case of the approximated potential (2.5). We set $\lambda = 3 \times 10^{-16}$, $f_\phi = 10^{16}$ GeV, and $m_\phi = 1$ eV, corresponding to $\theta_{\text{tr}} \simeq 1.4 \times 10^{-17}$.

dominated by the quartic term compared to the quadratic term. This can be understood by noting that the potential gets steeper as the quartic term dominates over the quadratic one.

In order to reach the BD distribution, we need a sufficiently large number of e -folds; $N \sim H_{\text{inf}}^2/m_\phi^2$ for the quadratic potential, and $N \sim 1/\sqrt{\lambda}$ for the quartic potential. Such a large number of e -folds can be realized by the eternal inflation [18–23] (see also [24–26]). Note that the eternity of the eternal inflation usually relies on the volume measure. Recently it was shown that a sufficiently large number of e -folds can be realized without relying on the volume measure, if one considers a hilltop-type stochastic inflation with a shallow local minimum around the potential maximum [27].

Lastly let us comment on the assumption that the probability distribution $P(\theta)$ is vanishingly small at $\theta = \pm\pi$ in the above discussion. The approximated expressions (3.10), (3.12), and (3.13) can only be applied to the case of $\theta_{\text{ini}} \ll \pi$, or equivalently, $H_{\text{inf}} \lesssim \Lambda$ and $\Lambda_{1,2}$. For $H_{\text{inf}} > \Lambda$ or $\Lambda_{1,2}$, the axion can go over the potential barrier due to the large fluctuations and all the physically inequivalent vacua will be populated as a result of the stochastic dynamics. For the potentials considered here, the asymptotic distribution will be almost uniform over the entire values of ϕ , and a typical value of the initial misalignment angle measured from the nearest minimum will be of order unity. Also, there is thermal radiation with the Gibbons-Hawking temperature $T_{\text{inf}} = H_{\text{inf}}/2\pi$ [28], which may significantly modify the axion potential if Λ or $\Lambda_{1,2}$ corresponds to the dynamical scale of the non-perturbative effects responsible for generating the axion potential. In the following, therefore, we will focus on the case of $\theta_{\text{ini}} \lesssim 1$, or equivalently, $H_{\text{inf}} \lesssim \Lambda_1$ or Λ .

3.2 Axion abundance

During inflation the axion follows the BD distribution derived in the previous subsection. After inflation, the axion starts to oscillate about the potential minimum when the effective mass, $|V''(\phi)|$, becomes comparable to the Hubble parameter.² In the case of the axion

² The commencement of oscillations is delayed if the initial position is close to the potential maximum, in which case the isocurvature perturbation as well as its non-Gaussianity are enhanced [29]. See also discussion

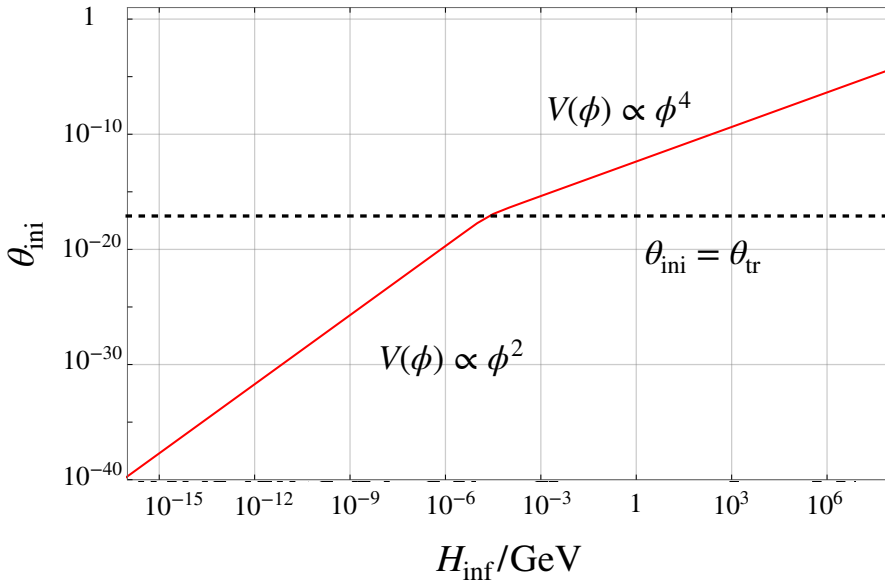


Figure 2. The initial angle θ_{ini} as a function of the inflation scale H_{inf} for $\Lambda_1 = 10^{12}$ GeV, $f_\phi = 10^{16}$ GeV, and $m_\phi = 1$ eV. The red line represents the initial angle which is estimated with the original potential (2.4). The horizontal dotted line is the transition point, $\theta_{\text{tr}} \simeq 1.4 \times 10^{-17}$.

potential (2.2), the axion coherent oscillations behave as cold dark matter. On the other hand, in the case of the axion potential (2.5), the axion coherent oscillations behave as radiation until the oscillation amplitude becomes so small that the tiny mass term comes to dominate the potential.

The final axion abundance depends on the oscillation amplitude, ϕ_{osc} , when the axion starts to oscillate. Here let us relate $\theta_{\text{osc}} \equiv \phi_{\text{osc}}/f_\phi$ to the initial angle θ_{ini} , following Refs. [15, 30]. We define the onset of the oscillation to be the time when the temporal variation of the axion field over the Hubble time becomes comparable to the distance to the potential minimum:

$$\left| H^{-1} \frac{\dot{\phi}}{\phi} \right|_{\text{osc}} \equiv \frac{1}{2}. \quad (3.14)$$

The choice of 1/2 in the right-handed side is just a convention, and it can be replaced with a constant of order unity.

Before the onset of the oscillation, the axion dynamics is described by an attractor solution of

$$cH\dot{\phi} \simeq -V', \quad (3.15)$$

where c is a numerical coefficient that depends on the equation of state of the dominant component of the universe,

$$c = \begin{cases} 3 & (\text{de Sitter}) \\ \frac{9}{2} & (\text{matter dominant}) \\ 5 & (\text{radiation dominant}) \end{cases}. \quad (3.16)$$

in Sec. 5.

Here the equation of motion is valid if $|V''| \ll H^2$. Using (3.14) and (3.15) we can express the Hubble parameter at the onset of oscillations in terms of ϕ_{osc} ,

$$H_{\text{osc}}^2 \simeq \frac{2V'(\phi_{\text{osc}})}{c_{\text{osc}}\phi_{\text{osc}}}, \quad (3.17)$$

where c_{osc} represents c evaluated at the onset of oscillations. For the quadratic and quartic potentials, it is given by

$$H_{\text{osc}} \simeq \begin{cases} \sqrt{\frac{2}{c_{\text{osc}}}} m_\phi & \text{(quadratic)} \\ \sqrt{\frac{\lambda}{3c_{\text{osc}}}} \phi_{\text{osc}} & \text{(quartic)}. \end{cases} \quad (3.18)$$

$$H_{\text{osc}} \simeq \begin{cases} \sqrt{\frac{2}{c_{\text{osc}}}} m_\phi & \text{(quadratic)} \\ \sqrt{\frac{\lambda}{3c_{\text{osc}}}} \phi_{\text{osc}} & \text{(quartic)}. \end{cases} \quad (3.19)$$

Integrating Eq. (3.15) from the end of inflation to the onset of oscillations, we obtain

$$\int_{\phi_{\text{ini}}}^{\phi_{\text{osc}}} \frac{d\phi}{V'} \simeq -\frac{1}{2c_{\text{osc}}(c_{\text{osc}} - 3)H_{\text{osc}}^2}, \quad (3.20)$$

where we have used $\dot{H}/H^2 = 3 - c$, and $H_{\text{osc}} \ll H_{\text{inf}}$. Then we can relate θ_{osc} to θ_{ini} for the quadratic and quartic potentials,

$$\theta_{\text{osc}} \simeq \theta_{\text{ini}} \times \begin{cases} \exp\left[-\frac{1}{4(c_{\text{osc}} - 3)}\right] & \text{(quadratic)} \\ \sqrt{\frac{2c_{\text{osc}} - 7}{2c_{\text{osc}} - 6}} & \text{(quartic)}, \end{cases} \quad (3.21)$$

$$\theta_{\text{osc}} \simeq \theta_{\text{ini}} \times \begin{cases} \exp\left[-\frac{1}{4(c_{\text{osc}} - 3)}\right] & \text{(quadratic)} \\ \sqrt{\frac{2c_{\text{osc}} - 7}{2c_{\text{osc}} - 6}} & \text{(quartic)}, \end{cases} \quad (3.22)$$

One can see that $\theta_{\text{osc}} \simeq \theta_{\text{ini}}$ in these cases. Since θ_{ini} is determined by the BD distribution in our scenario, the final axion abundance depends on the inflation scale, H_{inf} . Note that, in the previous work [15], the initial angle θ_{ini} was chosen in such a way that the curvature of the axion potential at $\theta = \theta_{\text{ini}}$ becomes comparable to the Hubble parameter during inflation. On the other hand, θ_{ini} is dynamically determined by the competition between the classical motion and quantum diffusion in our case. As a result, the initial angle is much smaller than assumed in the Ref. [15]. In the following we estimate the axion abundance for the quadratic and quartic potentials using the oscillation amplitude determined by the BD distribution.

3.2.1 The case of the quadratic potential

First, let us consider the case in which the axion potential is well approximated by the quadratic potential. This is the case either if the axion potential is given by a single cosine term (2.2) and the initial angle satisfies $\theta_{\text{ini}} \lesssim 1$, or if the potential is given by a flat-bottomed form (2.5) and θ_{ini} is smaller than θ_{tr} .

The axion abundance depends on whether the reheating is completed or not at the onset of oscillations. First, let us consider the case in which the axion starts to oscillate before the reheating. Taking account of the conservation of the entropy in the comoving volume after reheating, and the dependence of the axion energy density on the scale factor R , $\rho_\phi \propto R^{-3}$, the ratio of the axion energy density to the entropy density at present is given by

$$\left. \frac{\rho_\phi}{s} \right|_0 = \left. \frac{\rho_\phi}{s} \right|_{\text{reh}} = \left. \frac{\rho_{\text{inf}}}{s} \right|_{\text{reh}} \left. \frac{\rho_\phi}{\rho_{\text{inf}}} \right|_{\text{osc}} \simeq \frac{3T_{\text{reh}}}{4} \frac{\rho_{\phi,\text{osc}}}{3H_{\text{osc}}^2 M_{\text{Pl}}^2}, \quad (3.23)$$

where the subscripts, ‘0’, ‘reh’, and ‘osc’, imply that the variables are evaluated at present, reheating, and the onset of oscillations, respectively, and ρ_{inf} is the inflaton energy density. For simplicity we have assumed that the inflaton energy density decreases as non-relativistic matter before the reheating, and that the reheating takes place almost instantaneously at $T = T_{\text{reh}}$. The axion energy density at the onset of oscillations is given by

$$\rho_{\phi,\text{osc}} = \frac{1}{2}\dot{\phi}_{\text{osc}}^2 + \frac{1}{2}m_\phi^2\phi_{\text{osc}}^2 = \left(\frac{1}{4c} + \frac{1}{2}\right) m_\phi^2\phi_{\text{osc}}^2. \quad (3.24)$$

Using (3.10), (3.17), and (3.24), we can express the axion abundance in terms of the density parameter as

$$\Omega_\phi h^2 \simeq 0.39 \left(\frac{H_{\text{inf}}}{10^6 \text{ GeV}}\right)^4 \left(\frac{m_\phi}{1 \text{ GeV}}\right)^{-2} \left(\frac{T_{\text{reh}}}{10^6 \text{ GeV}}\right). \quad (3.25)$$

Here the density parameter is defined by $\Omega_\phi \equiv \rho_{\phi,0}/\rho_{\text{crit}}$, where $\rho_{\text{crit}} \simeq (0.0300 \text{ eV})^4 h^2$ is the critical density, and h is the reduced Hubble constant.

Next, we consider the case where the axion starts to oscillate after the reheating. The entropy density at the onset of the oscillations s_{osc} is given by $s_{\text{osc}} = (2\pi^2/45)g_*(T_{\text{osc}})T_{\text{osc}}^3$ in terms of the temperature T_{osc} ,

$$T_{\text{osc}} \equiv \left(\frac{\pi^2 g_*(T_{\text{osc}})}{90}\right)^{-\frac{1}{4}} \sqrt{H_{\text{osc}} M_{\text{Pl}}}, \quad (3.26)$$

$$\simeq 6.7 \times 10^8 \text{ GeV} \left(\frac{g_*(T_{\text{osc}})}{106.75}\right)^{-\frac{1}{4}} \left(\frac{m_\phi}{1 \text{ GeV}}\right)^{\frac{1}{2}}, \quad (3.27)$$

where g_* counts the effective relativistic degrees of freedom, and we substituted $c_{\text{osc}} = 5$ in the second equality. The axion abundance is given by

$$\Omega_\phi h^2 \simeq 0.19 \left(\frac{g_*(T_{\text{osc}})}{106.75}\right)^{-\frac{1}{4}} \left(\frac{H_{\text{inf}}}{10^5 \text{ GeV}}\right)^4 \left(\frac{m_\phi}{0.3 \text{ GeV}}\right)^{-\frac{3}{2}}. \quad (3.28)$$

Note that, although it is not explicitly shown in the final results, Ω_ϕ is proportional to θ_{ini}^2 in both cases. (The dependence on θ_{ini} can be inferred by noting $\theta_{\text{ini}} \propto H_{\text{inf}}^2$ in the case of the quadratic potential.)

3.2.2 The case of the quartic potential

Now we consider the flat-bottomed potential where the potential (2.5) consists of the quartic coupling plus a suppressed mass term. We focus on the case of $\theta_{\text{ini}} \simeq \theta_{\text{osc}} \gtrsim \theta_{\text{tr}}$ because otherwise the axion abundance is reduced to the case of the quadratic potential.

First, let us consider the case in which the axion starts to oscillate before the reheating. Noting that the axion energy density decreases as $\rho_\phi \propto R^{-4}$ until the quadratic term comes to dominate the potential, one can express the ratio of the axion energy density to the entropy density at present as

$$\left.\frac{\rho_\phi}{s}\right|_0 = \rho_{\phi,\text{tr}}^{1/4} \left.\frac{\rho_{\text{inf}}}{s}\right|_{\text{reh}} \left.\frac{\rho_\phi^{3/4}}{\rho_{\text{inf}}}\right|_{\text{osc}}. \quad (3.29)$$

Here $\rho_{\phi,\text{tr}}$ is the axion energy density when the oscillation amplitude becomes equal to $\phi_{\text{tr}} = \theta_{\text{tr}} f_\phi$, and it is given by

$$\rho_{\phi,\text{tr}} = \frac{9m_\phi^4}{2\lambda}. \quad (3.30)$$

The axion energy density at the onset of oscillations is

$$\rho_{\phi,\text{osc}} \simeq \frac{1}{2}\dot{\phi}_{\text{osc}}^2 + \frac{\lambda}{4!}\phi_{\text{osc}}^4 = \frac{\lambda}{4!} \left(1 + \frac{1}{c}\right) \phi_{\text{osc}}^4. \quad (3.31)$$

Thus, we arrive at the axion abundance,

$$\begin{aligned} \Omega_\phi h^2 &\simeq 0.50 \left(\frac{H_{\text{inf}}}{10^8 \text{ GeV}}\right) \left(\frac{m_\phi}{100 \text{ MeV}}\right) \left(\frac{f_\phi}{10^{16} \text{ GeV}}\right)^3 \\ &\times \left(\frac{\Lambda_1}{10^{12} \text{ GeV}}\right)^{-3} \left(\frac{T_{\text{reh}}}{10^{10} \text{ GeV}}\right). \end{aligned} \quad (3.32)$$

One can see that Ω_ϕ is proportional to θ_{ini} . Note that the axion abundance does not depend on the order of the reheating and the transition from the quartic to the quadratic potential.

Next, we consider the case in which the reheating precedes the onset of the axion oscillations. As before, the ratio of the axion energy density to the entropy density at present is given by

$$\left.\frac{\rho_\phi}{s}\right|_0 = \left.\frac{\rho_\phi}{s}\right|_{\text{tr}} = \rho_{\phi,\text{tr}}^{\frac{1}{4}} \frac{\rho_{\phi,\text{osc}}^{\frac{3}{4}}}{s_{\text{osc}}}. \quad (3.33)$$

where the temperature at the oscillation reads

$$T_{\text{osc}} \simeq 3.4 \times 10^{10} \text{ GeV} \left(\frac{g_*(T_{\text{osc}})}{106.75}\right)^{-\frac{1}{4}} \left(\frac{H_{\text{inf}}}{10^8 \text{ GeV}}\right)^{\frac{1}{2}} \left(\frac{f_\phi}{10^{16} \text{ GeV}}\right)^{-\frac{1}{2}} \left(\frac{\Lambda}{10^{12} \text{ GeV}}\right)^{\frac{1}{2}}. \quad (3.34)$$

Therefore, the axion abundance is obtained as

$$\begin{aligned} \Omega_\phi h^2 &\simeq 2.0 \left(\frac{g_*(T_{\text{osc}})}{106.75}\right)^{-\frac{1}{4}} \left(\frac{H_{\text{inf}}}{10^8 \text{ GeV}}\right)^{\frac{3}{2}} \left(\frac{m_\phi}{100 \text{ MeV}}\right) \\ &\times \left(\frac{f_\phi}{10^{16} \text{ GeV}}\right)^{\frac{5}{2}} \left(\frac{\Lambda_1}{10^{12} \text{ GeV}}\right)^{-\frac{5}{2}}. \end{aligned} \quad (3.35)$$

One can see that Ω_ϕ in this case is proportional to $\theta_{\text{ini}}^{\frac{3}{2}}$.

Note that the dependence of the axion abundance on the inflation scale is milder than the case of the quadratic potential (see Fig. 2). This as well as the tiny m_ϕ are the reason why the larger H_{inf} can be consistent with the dark matter abundance in the case of the quartic potential.

3.2.3 Thermal axion particle production

So far, we have considered the axion condensate. When the reheating temperature is sufficiently high, thermal axion particle production becomes important. If too many axion particles are produced, they contribute to hot or warm dark matter. Here let us estimate the

abundance of thermally produced axions. To this end, suppose for simplicity that the axion couples to weak gauge bosons as

$$\mathcal{L} = c_2 \frac{\alpha_2}{8\pi} \frac{\phi}{f_\phi} W_{\mu\nu}^a \tilde{W}_a^{\mu\nu} + c_Y \frac{\alpha_Y}{4\pi} \frac{\phi}{f_\phi} B_{\mu\nu} \tilde{B}^{\mu\nu}, \quad (3.36)$$

where $(\alpha_2, W_{\mu\nu}^a)$ and $(\alpha_Y, B_{\mu\nu})$ are the fine-structure constant and gauge field strength of $SU(2)_L$ and $U(1)_Y$, respectively, and c_2 and c_Y are model-dependent anomaly coefficients.³ Since they are higher dimensional terms, thermal production is efficient around the highest temperature, i.e. $T \sim T_{\text{reh}}$, in the radiation dominant era. Here we assume the instantaneous reheating for simplicity. The axion number density to entropy density is estimated

$$\frac{n_\phi^{\text{th}}}{s} \simeq r \frac{45\zeta(3)}{2g_*\pi^4} \quad (3.37)$$

where r was calculated in [31],

$$r \approx (3 \times 10^{-10} c_2^2 + 5 \times 10^{-11} c_Y^2) \left(\frac{10^{16} \text{ GeV}}{f_\phi} \right)^2 \left(\frac{T_{\text{reh}}}{10^{10} \text{ GeV}} \right). \quad (3.38)$$

One obtains the abundance of the thermally produced axion as

$$\Omega_\phi^{\text{th}} h^2 \simeq (2 \times 10^{-9} c_2^2 + 3 \times 10^{-10} c_Y^2) \left(\frac{m_\phi}{10 \text{ keV}} \right) \left(\frac{10^{16} \text{ GeV}}{f_\phi} \right)^2 \left(\frac{T_{\text{reh}}}{10^{10} \text{ GeV}} \right). \quad (3.39)$$

Thus, the thermal production is always subdominant for $c_2, c_Y = \mathcal{O}(1)$ in the parameter region that we will consider. However, it could be sizable when $T_{\text{reh}} \sim f_\phi$ or $c_2, c_Y \gg \mathcal{O}(1)$. Also, thermal production can be relevant if there are other interactions e.g. an axion-top quark interaction.

Notice that the above result applies to both potentials of (2.2) or (2.5) as long as Λ_1 or Λ is much smaller than f_ϕ . On the other hand, when Λ_1 in (2.5) is so large that the self-interaction of ϕ becomes important, the processes of $\phi\phi \leftrightarrow \phi\phi, \phi\phi \leftrightarrow \phi\phi\phi\phi$ may not be neglected. These processes increase the number density, while reducing the energy per one axion particle. Therefore in this case we can obtain much colder axion particles (if the processes are in equilibrium the typical temperature is $T_\phi \sim r^{1/4} T$) and their abundance is larger than the above estimate. For $\Lambda_1 \gg H_{\text{inf}}$, the contribution of coherent mode, (3.35), can be suppressed and thus thermally produced axions may explain the observed dark matter.⁴

4 Cosmological bounds

In this section, we study cosmological constraints on the axion dark matter in our scenario. Specifically we consider the axionic isocurvature perturbations and the diffuse X-ray/ γ -ray fluxes from the axion decays. By doing so we will be able to identify the viable parameter region where the axion explains the observed dark matter abundance.

³In the low energy effective theory in the broken phase, one obtains the coupling to photons, $\alpha_{\phi\gamma\gamma}$ defined in Eq. (4.11) as $\alpha_{\phi\gamma\gamma}/\alpha_{\text{EM}} = c_2/2 + c_Y$.

⁴In this case, the isocurvature bound is evaded.

4.1 Isocurvature perturbations

Since the axion is assumed to be light during inflation, it acquires quantum fluctuations of $\delta\phi_k \simeq H_{\text{inf}}/2\pi$ at the horizon exit, where k denotes the comoving wavenumber. This gives rise to the almost scale-invariant isocurvature perturbation, whose power spectrum is given by

$$\mathcal{P}_S = \left[\frac{\Omega_\phi}{\Omega_{\text{DM}}} \frac{\partial \ln \Omega_\phi}{\partial \theta_{\text{ini}}} \frac{\delta\phi_k}{f_\phi} \right]^2 = \left[p \frac{H_{\text{inf}}}{2\pi\theta_{\text{ini}}f_\phi} \right]^2, \quad (4.1)$$

where $\Omega_{\text{DM}} \simeq 0.12h^{-2}$ is the density parameter of the dark matter [1], and we have assumed $\Omega_\phi = \Omega_{\text{DM}}$ in the second equality. Here we have defined $p \equiv (\partial \ln \Omega_\phi / \partial \theta_{\text{ini}})$, and it is given by $p = 2$ for the quadratic potential, and $p = 1$ or $3/2$ for the quartic potential (cf. Sec. 3.2).

A mixture of isocurvature perturbations is tightly constrained by the Planck data. The current upper bound on the scale-invariant and uncorrelated isocurvature perturbation reads [32]

$$\mathcal{P}_S < 8.3 \times 10^{-11}. \quad (4.2)$$

In the following we derive the upper bound on the inflation scale as a function of the axion mass for the quadratic and quartic potential.

4.1.1 The case of the quadratic potential

Using (3.10) and $p = 2$, we obtain

$$\mathcal{P}_S = \frac{8m_\phi^2}{3H_{\text{inf}}^2} \simeq 2.7 \times 10^{-10} \left(\frac{H_{\text{inf}}}{10^5 \text{ GeV}} \right)^{-2} \left(\frac{m_\phi}{1 \text{ GeV}} \right)^2. \quad (4.3)$$

Thus, to satisfy the isocurvature bound (4.2), we need

$$H_{\text{inf}} \gtrsim 1.8 \times 10^5 m_\phi. \quad (4.4)$$

4.1.2 The case of the quartic potential

We focus on the case of $\theta_{\text{osc}} \gtrsim \theta_{\text{tr}}$ since otherwise the result will be reduced to the previous case. Using (3.12), we obtain

$$\mathcal{P}_S \simeq 0.14 p^2 \frac{\Lambda_1^2}{f_\phi^2} \simeq 0.079 p^2 \sqrt{\lambda}. \quad (4.5)$$

To satisfy the isocurvature bound (4.2), we need

$$\lambda \lesssim \frac{1.1 \times 10^{-18}}{p^4}. \quad (4.6)$$

Thus, the quartic coupling determines the size of isocurvature perturbations.

Since we assume $\Omega_\phi = \Omega_{\text{DM}}$, we can erase Λ_1 using (3.32) or (3.35) from the expression of \mathcal{P}_S . Then, we obtain

$$\mathcal{P}_S \simeq \begin{cases} 3.5 \times 10^{-9} \left(\frac{H_{\text{inf}}}{10^8 \text{ GeV}} \right)^{\frac{2}{3}} \left(\frac{m_\phi}{100 \text{ MeV}} \right)^{\frac{2}{3}} \left(\frac{T_{\text{reh}}}{10^{10} \text{ GeV}} \right)^{\frac{2}{3}} & (T_{\text{reh}} \lesssim T_{\text{osc}}) \quad (4.7) \\ 2.9 \times 10^{-8} \left(\frac{g_*(T_{\text{osc}})}{106.75} \right)^{-\frac{1}{5}} \left(\frac{H_{\text{inf}}}{10^8 \text{ GeV}} \right)^{\frac{6}{5}} \left(\frac{m_\phi}{100 \text{ MeV}} \right)^{\frac{4}{5}} & (T_{\text{osc}} \lesssim T_{\text{reh}}). \quad (4.8) \end{cases}$$

To satisfy the isocurvature bound (4.2), we need

$$H_{\text{inf}} \lesssim \begin{cases} 3.6 \times 10^5 \text{ GeV} \left(\frac{m_\phi}{100 \text{ MeV}} \right)^{-1} \left(\frac{T_{\text{reh}}}{10^{10} \text{ GeV}} \right)^{-1} & (T_{\text{osc}} \gtrsim T_{\text{reh}}) \\ 7.6 \times 10^5 \text{ GeV} \left(\frac{g_*(T_{\text{osc}})}{106.75} \right)^{\frac{1}{6}} \left(\frac{m_\phi}{100 \text{ MeV}} \right)^{-\frac{2}{3}} & (T_{\text{osc}} \lesssim T_{\text{reh}}). \end{cases} \quad (4.9)$$

In contrast to the quadratic potential, the isocurvature bound results in the upper bound on the inflation scale in the case of the quartic potential.

4.2 Axion decay into photons and hidden photons

The axion dark matter might have feeble interactions with the standard model or hidden sector particles. Here, we consider the axion-(hidden) photon couplings,

$$\frac{\alpha_{\phi\gamma\gamma}}{4\pi f_\phi} \phi F_{\mu\nu} \tilde{F}^{\mu\nu}, \quad \frac{\alpha_{\phi\gamma'\gamma'}}{4\pi f_\phi} \phi F'_{\mu\nu} \tilde{F}'^{\mu\nu}, \quad (4.11)$$

where $\alpha_{\phi\gamma\gamma}$ is a model-dependent coupling constant, $F_{\mu\nu}$ and $\tilde{F}^{\mu\nu}$ are the field strength of photons and its dual, respectively, and those with primes are for hidden photons.

First let us consider the axion decay into hidden photons through the above coupling. The decay rate is given by

$$\Gamma_\phi(\phi \rightarrow \gamma'\gamma') = \frac{\alpha_{\phi\gamma'\gamma'}^2 m_\phi^3}{64\pi^3 f_\phi^2}, \quad (4.12)$$

and if this is the dominant decay channel, the axion lifetime is given by

$$\tau_\phi(\phi \rightarrow \gamma'\gamma') \simeq 2.5 \times 10^{18} \text{ sec} \left(\frac{\alpha_{\phi\gamma'\gamma'}}{\alpha_{\text{EM}}} \right)^{-2} \left(\frac{m_\phi}{100 \text{ MeV}} \right)^{-3} \left(\frac{f_\phi}{10^{16} \text{ GeV}} \right)^2, \quad (4.13)$$

where $\alpha_{\text{EM}} \simeq 1/137$ is the electromagnetic fine-structure constant. The observational impact of dark matter decaying into dark radiation was studied in detail in Refs. [33, 34], and they placed a lower bound on the lifetime, $\tau_{\text{DM}} \geq 175 \text{ Gyr}$ [34]. This can be rewritten as the upper bound on the axion mass,

$$m_\phi \lesssim 76 \text{ MeV} \left(\frac{\alpha_{\phi\gamma'\gamma'}}{\alpha_{\text{EM}}} \right)^{-\frac{2}{3}} \left(\frac{f_\phi}{10^{16} \text{ GeV}} \right)^{\frac{2}{3}}. \quad (4.14)$$

Thus, for $f_\phi \simeq 10^{16} \text{ GeV}$ and $\alpha_{\phi\gamma'\gamma'} \simeq \alpha_{\text{EM}}$, the axion mass cannot exceed 80 MeV or so.

Next we consider the cosmological impact of the axion decay into ordinary photons. The energetic photons produced by the axion decay contribute to the Galactic and extra-galactic diffuse X-ray/ γ -ray background. First, let us estimate the Galactic halo contribution to the diffuse photon background [8, 35]. In order to derive the expected signal, we need the Galactic dark matter density profile. Here we assume the NFW dark matter profile [36, 37] and use the J-factor summarized in Table I of Ref. [35]. As we consider the axion-photon interaction (4.11), the produced two photons initially have the monochromatic spectrum

$$\frac{dN_\gamma}{dE_\gamma} = 2\delta \left(E_\gamma - \frac{m_\phi}{2} \right), \quad (4.15)$$

where E_γ and N_γ are the present photon energy and number, respectively. Then, the differential photon flux from the axion decay in the Milky Way is written by

$$\frac{d\Phi_{\text{MW}}}{dE_\gamma} = \int_{l.o.s} dy \frac{\Gamma_{\phi\gamma\gamma}}{4\pi y^2} \frac{dN_\gamma}{dE_\gamma} \frac{\rho_\phi(y)}{m_\phi} y^2 d\Omega = \frac{r_\odot}{4\pi} \frac{\rho_\odot}{m_\phi} \Gamma_{\phi\gamma\gamma} \frac{dN_\gamma}{dE_\gamma} \frac{\Omega_\phi}{\Omega_{\text{DM}}} J_{\text{D}}, \quad (4.16)$$

where $r_\odot = 8.5\text{kpc}$ is the distance between the Sun and the center of our Galaxy, $\rho_\odot = 0.3\text{GeV}/\text{cm}^3$ is the local dark matter density, ρ_ϕ is the axion energy density, and we define a J-factor as

$$J_{\text{D}} \equiv \int_{l.o.s} \frac{dy}{r_\odot} \frac{\rho_{\text{DM}}(y)}{\rho_\odot} d\Omega, \quad (4.17)$$

where ρ_{DM} represents a dark matter density profile. Here, the integration is taken over the observed region of the sky $\Delta\Omega$ and the line-of-sight distance y .

Let us next consider the extra-galactic contributions [38]. The photons coming from cosmological distances suffer a redshift due to the cosmic expansion. Also, the dark matter density in the early universe was higher than present density. Assuming the spatially homogeneous distribution of the axion, we obtain the photon flux per a unit solid angle

$$\frac{d^2\Phi_{\text{EG}}}{d\Omega dE_\gamma} = \frac{\Gamma_{\phi\gamma\gamma}}{4\pi} \int_{t_{\text{rec}}}^{t_0} d\tilde{t} n_\phi(\tilde{t}) (1+z)^{-3} \frac{d\tilde{E}_\gamma}{dE_\gamma} \frac{dN_\gamma}{d\tilde{E}_\gamma}, \quad (4.18)$$

where t_{rec} is the time of the recombination, z is the redshift parameter corresponding to the time $t = \tilde{t}$, \tilde{E}_γ is the photon energy at the production, and the axion density $n_\phi(\tilde{t})$ is defined by

$$n_\phi(\tilde{t}) \equiv n_{\phi,0} (1+z)^3 = \frac{\Omega_\phi \rho_{\text{crit}}}{m_\phi} (1+z)^3. \quad (4.19)$$

Here, we have neglected a slight decrease of the axion density due to the decay, because the lifetime must be much longer than the present age of the universe. Note that we put a cut-off at recombination, since photons cannot propagate freely until the recombination. The redshift parameter z is related to the cosmic time t by

$$\frac{dt}{dz} = - \left[H_0 (1+z) \sqrt{\Omega_m (1+z)^3 + \Omega_\Lambda} \right]^{-1}, \quad (4.20)$$

where H_0 is the Hubble constant, and Ω_m and Ω_Λ denote the density parameter of non-relativistic matter and the cosmological constant, respectively. Using this relation in the integration (4.18), we obtain the extra-galactic photon flux per a unit solid angle,

$$\frac{d^2\Phi_{\text{EG}}}{d\Omega dE_\gamma} = \frac{\Omega_\phi \rho_{\text{crit}} \Gamma_{\phi\gamma\gamma}}{2\pi m_\phi E_\gamma H_0} \left[\Omega_\Lambda + \Omega_m \left(\frac{m_\phi}{2E_\gamma} \right)^3 \right]^{-1/2}. \quad (4.21)$$

Since we can observe photons produced after the recombination, the energy E_γ is in the range of $\frac{m_\phi}{2}/(1+z_{\text{rec}}) < E_\gamma < \frac{m_\phi}{2}$, where $z_{\text{rec}} \simeq 1100$.

The constraint is placed on the parameters by the fact that the two contributions (4.16) and (4.21) should be smaller than the observational flux F_{obs} . In this work, we compare the values integrated in the range of each energy bin width ΔE_γ with the observed flux,

$$\int_{\Delta E_\gamma} dE_\gamma \left[\frac{1}{\Delta\Omega} E_\gamma^2 \frac{d\Phi_{\text{MW}}}{dE_\gamma} + E_\gamma^2 \frac{d^2\Phi_{\text{EG}}}{d\Omega dE_\gamma} \right] \lesssim F_{\text{obs}} \Delta E_\gamma, \quad (4.22)$$

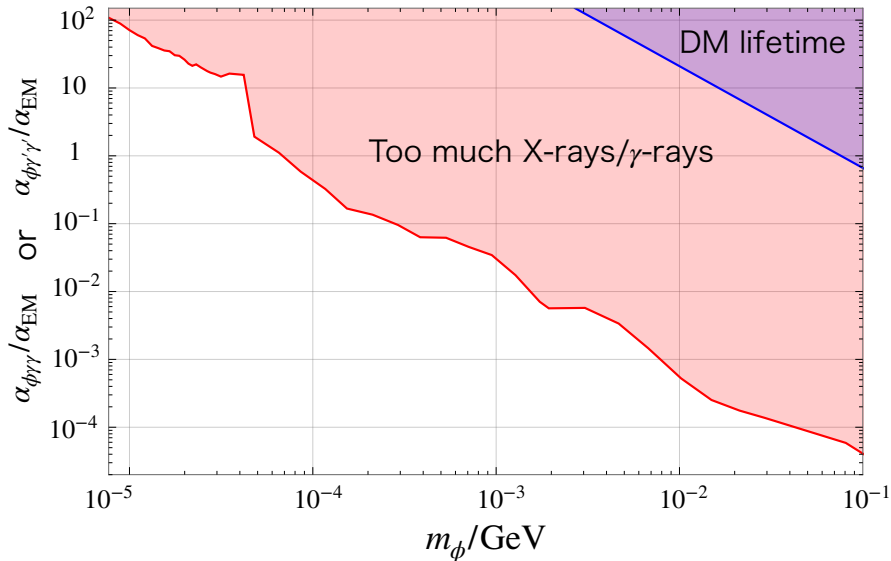


Figure 3. The observational constraints on the axion coupling to photons and hidden photons. The shaded regions are excluded, and we set $f_\phi = 10^{16}$ GeV. The red shaded region denotes the constraint (4.22) from the axion decay into photons, and the blue region is the constraint (4.14) from the invisible decay of axion dark matter.

where the unit $[\text{MeVcm}^{-2}\text{s}^{-1}\text{sr}^{-1}]$ of the photon flux is used in our analysis. We used the observational results from HEAO-1, INTEGRAL, COMPTEL, and EGRET summarized in [35]. The results are shown in Fig. 3 where we set $f_\phi = 10^{16}$ GeV. The red region represents the constraint (4.22) from the diffuse photon spectrum from the axion decay. The blue region is the constraint (4.14) from the dark matter lifetime. For $\alpha_{\phi\gamma\gamma} = \alpha_{\text{EM}}$, the axion mass has an upper bound $m_\phi \lesssim 70$ keV.

4.3 Primordial tensor mode

During inflation the primordial tensor mode, i.e. primordial gravitational waves, are generated, which contribute to the CMB temperature and polarization anisotropies. Its amplitude is proportional to the inflation scale H_{inf} . The absence of the primordial tensor mode so far in the CMB observations by Planck and BICEP2/Keck Array provides an upper bound on H_{inf} [32]:

$$H_{\text{inf}} < 6.5 \times 10^{13} \text{ GeV} \quad (95\% \text{ C.L.}). \quad (4.23)$$

4.4 Results

Combining the above cosmological bounds, we show in Fig. 4 the viable parameter space on the (m_ϕ, H_{inf}) plane as a white region where the axion explains all dark matter. Here we fix $f_\phi = 10^{16}$ GeV and $T_{\text{reh}} = 10^{10}$ GeV, and choose an appropriate value of Λ_1 for each m_ϕ and H_{inf} to realize $\Omega_\phi = \Omega_{\text{DM}}$. In the lower right gray region, θ_{ini} is smaller than θ_{tr} , and the axion dynamics is same as for the quadratic potential, and the axion abundance is independent of Λ_1 . On the boundary line, the axion explains all dark matter, while the axion abundance is smaller than the observed dark matter abundance below the gray line. The purple and blue shaded regions are excluded by the absence of the tensor and isocurvature perturbations

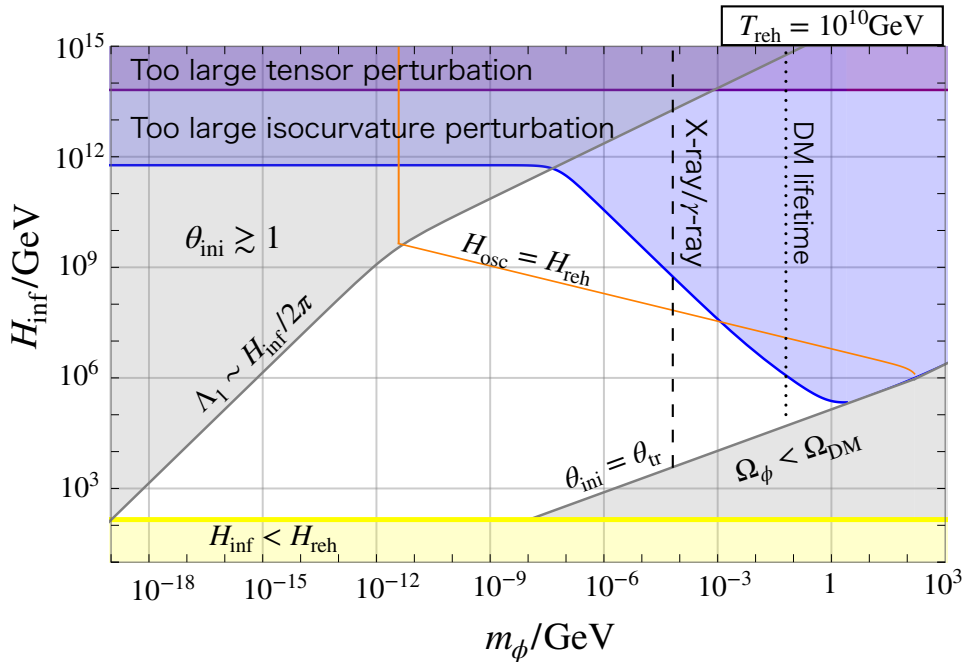


Figure 4. The viable parameter space shown as a white region where $\Omega_\phi = \Omega_{\text{DM}}$. We set $f_\phi = 10^{16}$ GeV, and $T_{\text{reh}} = 10^{10}$ GeV. The lower-right gray line shows $\theta_{\text{ini}} = \theta_{\text{tr}}$ below which the axion abundance falls short of the observed dark matter abundance. The purple and blue regions are the bounds from the absence of the primordial tensor mode (4.23) and the isocurvature perturbation (4.9) and (4.10), respectively. The yellow region does not satisfy the condition that the reheating follows the inflation. The dotted vertical line is the constraint from the axion decay into hidden photons for $\alpha_{\phi\gamma'\gamma'} = \alpha_{\text{EM}}$ and the dashed line is the constraint from the X-ray/ γ -ray diffuse flux for $\alpha_{\phi\gamma\gamma} = \alpha_{\text{EM}}$. The upper left gray region represents $\theta_{\text{ini}} \gtrsim 1$. The orange solid line is the boundary $H_{\text{reh}} = H_{\text{osc}}$. Note that the quadratic case corresponds to the lower right gray region.

(4.23), (4.9) and (4.10), respectively. The yellow shaded region at the bottom is excluded because of $H_{\text{reh}} > H_{\text{inf}}$. The dotted vertical line represents a constraint $m_\phi \lesssim 80$ MeV, which comes from the invisible axion decay into hidden photons for $\alpha_{\phi\gamma'\gamma'} = \alpha_{\text{EM}}$, while the dashed line represents the constraint $m_\phi \lesssim 70$ keV from the X-ray/ γ -ray diffuse flux for $\alpha_{\phi\gamma\gamma} = \alpha_{\text{EM}}$. In the upper left gray region, θ_{ini} given in Eq. (3.13) would become larger than unity, and our approximated potential is no longer justified. The isocurvature bound in this region is calculated assuming $\theta_{\text{ini}} = 1$. Above the orange solid line, the axion starts to oscillate before the reheating, i.e., $H_{\text{osc}} > H_{\text{reh}}$. The cases for $T_{\text{reh}} = 10^7$ and 10^{13} GeV are also shown in Fig. 5. In the upper panel with $T_{\text{reh}} = 10^7$ GeV, the red line denotes $H_{\text{reh}} = H_{\text{tr}}$. In the right to the red line, the reheating takes place after the oscillation amplitude becomes smaller than ϕ_{tr} , $H_{\text{reh}} \lesssim H_{\text{tr}} \lesssim H_{\text{osc}}$.

As mentioned above, in the quadratic case, a right amount of dark matter can be explained on the boundary line of the lower right gray region. The allowed region shown as a becomes much larger in the case of the quartic potential. This is because, for a given inflation scale, the initial angle θ_{ini} becomes smaller and the axion abundance behaves like radiation and therefore decreases faster in the quartic case than in the quadratic case. In particular, the reheating temperature can be as high as $T_{\text{reh}} \lesssim 10^{14}$ GeV. Thermal leptogenesis works for such a high reheating temperature [39]. For some range of the axion mass, the upper bound

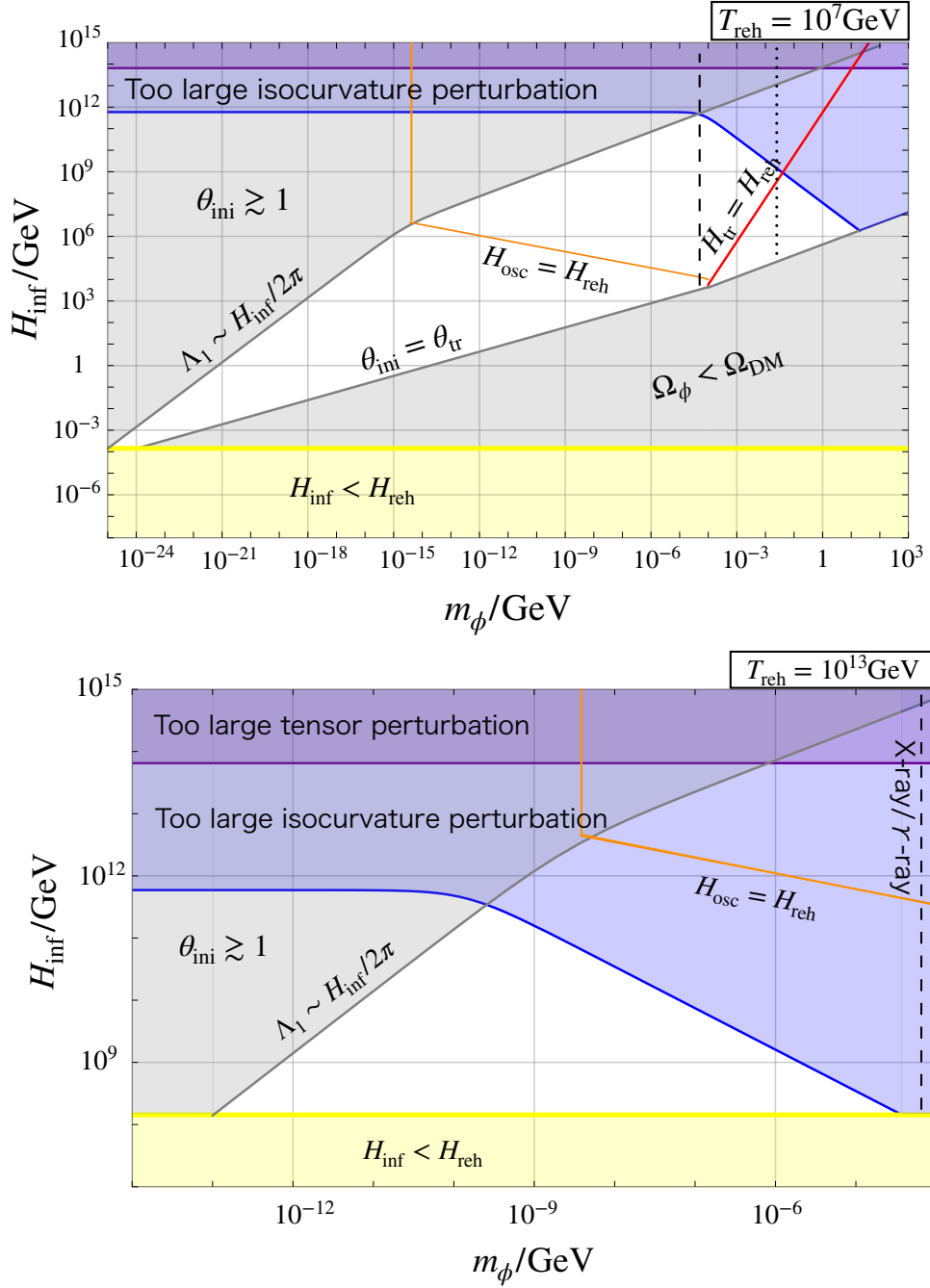


Figure 5. Same as Fig. 4 but for $T_{\text{reh}} = 10^7 \text{ GeV}$ (upper) and $T_{\text{reh}} = 10^{13} \text{ GeV}$ (lower). In the upper panel, the red line denotes $H_{\text{reh}} = H_{\text{tr}}$.

on the inflation scale is given by the isocurvature bound, and so, future CMB observations will be able to probe the corresponding parameter space. In addition, the relatively heavy axion dark matter with mass $m_\phi \sim 10^{-6} - 1 \text{ GeV}$ can be realized by virtue of the BD distribution. Therefore, if the axion couples to two photons, next-generation gamma-ray satellites such as AMEGO [40, 41] and eASTROGAM [42] will improve the bound significantly. If the axion

mainly couples to the hidden photons (or other hidden light particles), on the other hand, the present scenario may be probed by further observations of the present and late-time universe (cf. Refs. [33, 34]). In particular, the decaying dark matter may ameliorate the H_0 tension [43].

5 Delayed onset of oscillations and π inflation

So far we have focused on a case in which the axion mass at the minimum is suppressed compared to the typical curvature scale of the potential. In this section we consider another possibility that the axion potential has a plateau region away from the minimum which delays the onset of oscillation. Such a possibility was extensively studied in the literature, because coherent oscillations in a potential flatter than the quadratic one leads to spatial instabilities, formation of non-topological solitons such as oscillons/I-balls [44–46] (see also Refs. [47–58] for more details about the formation and decay processes in various contexts) and the production of the gravitational waves [59–61]. Also, the delayed onset of oscillations enhances the final axion abundance as well as its isocurvature perturbation (see the footnote 2.) The enhancement of the axion (or ALP) abundance can also be obtained by e.g. the adiabatic conversion between the axion and the QCD axion [62–65].

Here we present a model in which the initial value of the axion is set on the plateau of the potential in the stochastic axion scenario. If we consider only the dynamics of the light axion, the inflation scale H_{inf} must be higher than the height of the plateau, since otherwise the probability distribution of the axion would be peaked at the potential minimum and it is unlikely to find the axion on the plateau of the potential. However, if there is another heavy axion field that mixes with the light axion, the probability distribution of the lighter one can be shifted due to the heavy axion dynamics. Such a phase shift was recently used to realize a hilltop initial condition for the QCD axion [66, 67]. (see also Ref. [68] which uses the stronger QCD in the early Universe [69–72]).

Let us introduce another heavy axion field, ϕ_H , that mixes with the light axion. This is naturally realized in the axion landscape. We also assume that the location of the local maxima and minima of the heavy axion potential is the same as (or very close to) that of a single cosine term. For instance, this is the case if the heavy axion potential is dominated by a single cosine term, and another relatively small shift-symmetry breaking term(s) lifts the degeneracy of the vacua. Then, the universe may be first trapped in a false vacuum, and then tunnels to the adjacent lower vacuum, resulting in a field change by approximately 2π [66]. Alternatively, if the heavy axion plays a role of the inflaton, we need at least two cosine terms as long as we consider decay constants smaller than the Planck mass. Their relative height and phase are chosen so that the second cosine term makes the potential maximum of the first one sufficiently flat for successful slow-roll inflation to occur. Then, the field distance between the potential maximum and minimum is given by (a fraction of) π . This is due to the requirement of successful hilltop inflation. In either case, by introducing a certain mixing with the light axion, one can realize a phase shift of π . In particular, such inflation model that causes the phase shift of π was named π inflation [67].

To be concrete, let us consider the following potential for the light and heavy axions,

$$V_L(\phi, \theta_H) = \Lambda_1^4 \left[1 + \cos \left(\frac{\phi}{f_\phi} + \theta_H \right) \right] + \Lambda_2^4 \left[1 - \cos \left(2 \left(\frac{\phi}{f_\phi} + \theta_H \right) \right) \right], \quad (5.1)$$

where we assume $\Lambda_1^4 \simeq 4\Lambda_2^4$ as before, and $\theta_H \equiv \phi_H/f_H$ with f_H being the decay constant is the dimensionless angle corresponding to the heavy axion. We assume that the heavy axion

has its own potential satisfying the above mentioned property so that θ_H changes from 0 during inflation to π after inflation. We also assume that back reaction of $V_L(\phi, \theta_{\text{inf}})$ to the heavy axion dynamics is negligibly small.

During inflation the potential for ϕ is well approximated by the quadratic term around one of the minima, $\phi = \pi f_\phi$,

$$V_L(\phi, 0) \simeq \frac{1}{2} M_\phi^2 (\phi - \pi f_\phi)^2 \quad (\phi \sim \pi f_\phi). \quad (5.2)$$

where $M_\phi^2 \simeq (\Lambda_1^4 + 4\Lambda_2^4)/f_\phi^2$ is the effective mass during inflation. We assume $M_\phi \ll H_{\text{inf}} \ll \Lambda_1$ and the BD distribution of ϕ is reached after a sufficiently long inflation. The BD distribution of ϕ implies that $|\phi - \pi f_\phi| \sim H_{\text{inf}}^2/M_\phi$, and it is peaked at $\phi = \pi f_\phi$.

After inflation only the first term of the axion potential V_L receives the phase shift of π , since the second one remains the same after the phase shift of 2π . Then, the potential has a plateau around $\phi = \pi f_\phi$, and the minimum is shifted to the origin. If the typical time scale of the heavy axion dynamics is much shorter than M_ϕ^{-1} , the distribution of the light axion remains almost the intact, and it is still peaked at $\phi = \pi f_\phi$. The potential can be expanded again around $\phi = \pi f_\phi$ which is now the potential maximum,

$$V_L(\phi, \pi) \simeq 2\Lambda_1^4 - \frac{1}{2} m_\phi^2 (\phi - \pi f_\phi)^2 - \frac{\lambda}{4!} (\phi - \pi f_\phi)^4 + \dots \quad (\phi \sim \pi f_\phi) \quad (5.3)$$

On the other hand, the potential at around the minimum, $\phi = 0$, is approximately given by

$$V_L(\phi, \pi) \simeq \frac{1}{2} M_\phi^2 \phi^2 \quad (\phi \sim 0). \quad (5.4)$$

For simplicity let us assume that the axion is initially in the vicinity of $\phi = \pi f_\phi$ where the potential is dominated by the (negative) quadratic term, i.e., $|\theta_{\text{ini}} - \pi| \ll \theta_{\text{tr}}$ (see Eq. (2.8) for the definition of θ_{tr}), and that the reheating occurs instantaneously just after inflation, i.e., $H_{\text{inf}} \simeq H_{\text{reh}} > H_{\text{osc}}$. Then, one can determine the onset of oscillations from Eq. (3.20),

$$H_{\text{osc}} \sim \sqrt{\frac{\lambda}{60}} \theta_{\text{tr}} f_\phi, \quad (5.5)$$

where we have used $c_{\text{osc}} = 5$, and we have neglected the logarithmic contributions from the quadratic terms for simplicity. One finds that H_{osc} is not sensitive to θ_{ini} , and it is of order m_ϕ . After the axion starts to oscillate, the oscillation amplitude becomes smaller due to the cosmic expansion, and its oscillation frequency is determined by M_ϕ . One gets the abundance of the axion by taking $\Lambda_1^4 \simeq 4\Lambda_2^4$,

$$\Omega_\phi h^2 \sim 0.5 \left(\frac{M_\phi}{0.1 \text{ eV}} \right)^{\frac{1}{4}} \left(\frac{f_\phi}{10^6 \text{ GeV}} \right)^{\frac{7}{4}} \left(\frac{\theta_{\text{tr}}}{10^{-7}} \right)^{-3/2}. \quad (5.6)$$

Consequently we get the light axion dark matter with a very small decay constant. The onset of the oscillation happens at $T \sim 10 \text{ GeV}$ and the potential height is $\Lambda_1 \simeq 80 \text{ MeV}$. Here the small θ_{tr} controls the flatness of the plateau near $\phi = \pi f_\phi$, and therefore, the enhancement of the axion abundance. To have $\theta_{\text{ini}} < \theta_{\text{tr}} \sim 10^{-7}$, the Hubble parameter should be smaller than $\mathcal{O}(1) \text{ MeV}$.⁵ The isocurvature bound as well as the other constraints can be satisfied. Interestingly, such a light axion dark matter with $M_\phi \sim 0.01 - 1 \text{ eV}$ and $f_\phi \sim 10^6 - 10^7 \text{ GeV}$ can be searched in the IAXO experiment [75–77] or the PTOLEMY experiment [78–80] if the axion couples to photons or neutrinos.

⁵Such low-scale inflation and successful reheating can be realized in the ALP inflation [66, 73, 74].

6 Conclusions

We have studied the stochastic axion dark matter in the axion landscape that consists of many axions which generically have mass and kinetic mixings. Because of the various shift symmetry breaking terms as well as mass mixings, we expect that some of the axion potential and its dynamics may not be captured by the usual analysis based on a single cosine or a simple quadratic potential. In this paper, therefore, we have considered a possibility that the axion dynamics as well as its abundance are significantly affected by the deviation from the simple quadratic potential.

First, we have focused on a possibility that one of the light axions is responsible for the observed dark matter. In order to be sufficiently long-lived, the axion mass must be much lighter than the fundamental scale. This is realized either if there is a flat direction(s) in the landscape along which the typical curvature of the potential is very small, or if the axion mass happens to be suppressed around the potential minimum. In the latter case, the potential is well approximated by the suppressed quadratic term plus a quartic term. We have carefully studied the axion initial condition determined by the stochastic dynamics and its subsequent evolution after inflation. By taking account of various cosmological bounds, we have delineated the viable parameter region in Figs. 4 and 5. We have found that the axion dark matter can be realized for a broad region of the inflation scale and the axion mass; e.g. $H_{\text{inf}} = \mathcal{O}(10^{2-12})$ GeV and $m_\phi = 10^{-19} - 1$ GeV for $f_\phi = 10^{16}$ GeV and $T_{\text{reh}} = 10^{10}$ GeV.

We also discussed a case where the axion potential has a plateau away from the minimum, which delays the onset of oscillations. In particular we have shown that one can realize the axion probability distribution peaked at the plateau region by using the phase shift of π induced by the heavy axion dynamics. This is the so-called π inflation mechanism. Since the axion abundance can be significantly enhanced in this case, one can explain the observed dark matter density for a very small f_ϕ , e.g. $f_\phi = 10^6$ GeV and the axion mass of $\mathcal{O}(0.1 - 1)$ eV. Such axion dark matter with a small f_ϕ may be probed by the IAXO or PTOLEMY experiments if it has a coupling to photons or neutrinos.

Acknowledgments

This work is supported by JSPS KAKENHI Grant Numbers JP15H05889 (F.T.), JP15K21733 (F.T.), JP17H02875 (F.T.), JP17H02878 (F.T.), by World Premier International Research Center Initiative (WPI Initiative), MEXT, Japan, and by NRF Strategic Research Program NRF-2017R1E1A1A01072736 (W.Y.). One of us (S.N.) acknowledges support from the Graduate Program on Physics for the Universe (GP-PU) at Tohoku University.

References

- [1] PLANCK collaboration, N. Aghanim et al., *Planck 2018 results. VI. Cosmological parameters*, [1807.06209](#).
- [2] J. Preskill, M. B. Wise and F. Wilczek, *Cosmology of the Invisible Axion*, *Phys. Lett.* **120B** (1983) 127.
- [3] L. F. Abbott and P. Sikivie, *A Cosmological Bound on the Invisible Axion*, *Phys. Lett.* **120B** (1983) 133.

- [4] M. Dine and W. Fischler, *The Not So Harmless Axion*, *Phys. Lett.* **120B** (1983) 137.
- [5] P. W. Graham and A. Scherlis, *Stochastic axion scenario*, *Phys. Rev.* **D98** (2018) 035017 [[1805.07362](#)].
- [6] F. Takahashi, W. Yin and A. H. Guth, *QCD axion window and low-scale inflation*, *Phys. Rev.* **D98** (2018) 015042 [[1805.08763](#)].
- [7] T. S. Bunch and P. C. W. Davies, *Quantum Field Theory in de Sitter Space: Renormalization by Point Splitting*, *Proc. Roy. Soc. Lond.* **A360** (1978) 117.
- [8] S.-Y. Ho, F. Takahashi and W. Yin, *Relaxing the Cosmological Moduli Problem by Low-scale Inflation*, *JHEP* **04** (2019) 149 [[1901.01240](#)].
- [9] T. Higaki and F. Takahashi, *Natural and Multi-Natural Inflation in Axion Landscape*, *JHEP* **07** (2014) 074 [[1404.6923](#)].
- [10] T. Higaki and F. Takahashi, *Axion Landscape and Natural Inflation*, *Phys. Lett.* **B744** (2015) 153 [[1409.8409](#)].
- [11] G. Wang and T. Battefeld, *Vacuum Selection on Axionic Landscapes*, *JCAP* **1604** (2016) 025 [[1512.04224](#)].
- [12] A. Masoumi and A. Vilenkin, *Vacuum statistics and stability in axionic landscapes*, *JCAP* **1603** (2016) 054 [[1601.01662](#)].
- [13] P. Nath and M. Piskunov, *Evidence for Inflation in an Axion Landscape*, *JHEP* **03** (2018) 121 [[1712.01357](#)].
- [14] M. Yamada and A. Vilenkin, *Hessian eigenvalue distribution in a random Gaussian landscape*, *JHEP* **03** (2018) 029 [[1712.01282](#)].
- [15] R. Daido, T. Kobayashi and F. Takahashi, *Dark Matter in Axion Landscape*, *Phys. Lett.* **B765** (2017) 293 [[1608.04092](#)].
- [16] J. E. Kim, H. P. Nilles and M. Peloso, *Completing natural inflation*, *JCAP* **0501** (2005) 005 [[hep-ph/0409138](#)].
- [17] K. Choi, H. Kim and S. Yun, *Natural inflation with multiple sub-Planckian axions*, *Phys. Rev.* **D90** (2014) 023545 [[1404.6209](#)].
- [18] A. D. Linde, *NONSINGULAR REGENERATING INFLATIONARY UNIVERSE*, .
- [19] P. J. Steinhardt, *NATURAL INFLATION*, in *Nuffield Workshop on the Very Early Universe Cambridge, England, June 21-July 9, 1982*, pp. 251–266, 1982.
- [20] A. Vilenkin, *The Birth of Inflationary Universes*, *Phys. Rev.* **D27** (1983) 2848.
- [21] A. D. Linde, *ETERNAL CHAOTIC INFLATION*, *Mod. Phys. Lett.* **A1** (1986) 81.
- [22] A. D. Linde, *Eternally Existing Selfreproducing Chaotic Inflationary Universe*, *Phys. Lett.* **B175** (1986) 395.
- [23] A. S. Goncharov, A. D. Linde and V. F. Mukhanov, *The Global Structure of the Inflationary Universe*, *Int. J. Mod. Phys.* **A2** (1987) 561.
- [24] A. H. Guth, *Inflation and eternal inflation*, *Phys. Rept.* **333** (2000) 555 [[astro-ph/0002156](#)].
- [25] A. H. Guth, *Eternal inflation and its implications*, *J. Phys.* **A40** (2007) 6811 [[hep-th/0702178](#)].
- [26] A. Linde, *A brief history of the multiverse*, *Rept. Prog. Phys.* **80** (2017) 022001 [[1512.01203](#)].
- [27] N. Kitajima, Y. Tada and F. Takahashi, *Stochastic inflation with an extremely large number of e-folds*, *Phys. Lett.* **B800** (2020) 135097 [[1908.08694](#)].
- [28] G. W. Gibbons and S. W. Hawking, *Cosmological Event Horizons, Thermodynamics, and Particle Creation*, *Phys. Rev.* **D15** (1977) 2738.

- [29] T. Kobayashi, R. Kurematsu and F. Takahashi, *Isocurvature Constraints and Anharmonic Effects on QCD Axion Dark Matter*, *JCAP* **1309** (2013) 032 [[1304.0922](#)].
- [30] M. Kawasaki, T. Kobayashi and F. Takahashi, *Non-Gaussianity from Curvatons Revisited*, *Phys. Rev.* **D84** (2011) 123506 [[1107.6011](#)].
- [31] A. Salvio, A. Strumia and W. Xue, *Thermal axion production*, *JCAP* **1401** (2014) 011 [[1310.6982](#)].
- [32] PLANCK collaboration, Y. Akrami et al., *Planck 2018 results. X. Constraints on inflation*, [1807.06211](#).
- [33] K. Enqvist, S. Nadathur, T. Sekiguchi and T. Takahashi, *Decaying dark matter and the tension in σ_8* , *JCAP* **1509** (2015) 067 [[1505.05511](#)].
- [34] K. Enqvist, S. Nadathur, T. Sekiguchi and T. Takahashi, *Constraints on decaying dark matter from weak lensing and cluster counts*, [1906.09112](#).
- [35] R. Essig, E. Kuflik, S. D. McDermott, T. Volansky and K. M. Zurek, *Constraining Light Dark Matter with Diffuse X-Ray and Gamma-Ray Observations*, *JHEP* **11** (2013) 193 [[1309.4091](#)].
- [36] J. F. Navarro, C. S. Frenk and S. D. M. White, *The Structure of cold dark matter halos*, *Astrophys. J.* **462** (1996) 563 [[astro-ph/9508025](#)].
- [37] J. F. Navarro, C. S. Frenk and S. D. M. White, *A Universal density profile from hierarchical clustering*, *Astrophys. J.* **490** (1997) 493 [[astro-ph/9611107](#)].
- [38] T. Asaka, J. Hashiba, M. Kawasaki and T. Yanagida, *Cosmological moduli problem in gauge mediated supersymmetry breaking theories*, *Phys. Rev.* **D58** (1998) 083509 [[hep-ph/9711501](#)].
- [39] M. Fukugita and T. Yanagida, *Baryogenesis Without Grand Unification*, *Phys. Lett.* **B174** (1986) 45.
- [40] A. Moiseev and O. B. O. T. A. Team, *All-Sky Medium Energy Gamma-ray Observatory (AMEGO)*, *PoS ICRC2017* (2018) 798.
- [41] AMEGO collaboration, R. Caputo et al., *All-sky Medium Energy Gamma-ray Observatory: Exploring the Extreme Multimessenger Universe*, [1907.07558](#).
- [42] e-ASTROGAM collaboration, M. Tavani et al., *Science with e-ASTROGAM: A space mission for MeV-GeV gamma-ray astrophysics*, *JHEAp* **19** (2018) 1 [[1711.01265](#)].
- [43] A. G. Riess et al., *Milky Way Cepheid Standards for Measuring Cosmic Distances and Application to Gaia DR2: Implications for the Hubble Constant*, *Astrophys. J.* **861** (2018) 126 [[1804.10655](#)].
- [44] M. Gleiser, *Pseudostable bubbles*, *Phys. Rev.* **D49** (1994) 2978 [[hep-ph/9308279](#)].
- [45] E. J. Copeland, M. Gleiser and H. R. Muller, *Oscillons: Resonant configurations during bubble collapse*, *Phys. Rev.* **D52** (1995) 1920 [[hep-ph/9503217](#)].
- [46] S. Kasuya, M. Kawasaki and F. Takahashi, *I-balls*, *Phys. Lett.* **B559** (2003) 99 [[hep-ph/0209358](#)].
- [47] J. McDonald, *Inflaton condensate fragmentation in hybrid inflation models*, *Phys. Rev.* **D66** (2002) 043525 [[hep-ph/0105235](#)].
- [48] M. A. Amin and D. Shirokoff, *Flat-top oscillons in an expanding universe*, *Phys. Rev.* **D81** (2010) 085045 [[1002.3380](#)].
- [49] M. A. Amin, R. Easther, H. Finkel, R. Flauger and M. P. Hertzberg, *Oscillons After Inflation*, *Phys. Rev. Lett.* **108** (2012) 241302 [[1106.3335](#)].
- [50] M. A. Amin, *K-oscillons: Oscillons with noncanonical kinetic terms*, *Phys. Rev.* **D87** (2013) 123505 [[1303.1102](#)].

- [51] N. Takeda and Y. Watanabe, *No quasistable scalaron lump forms after R^2 inflation*, *Phys. Rev. D* **D90** (2014) 023519 [[1405.3830](#)].
- [52] M. Kawasaki, F. Takahashi and N. Takeda, *Adiabatic Invariance of Oscillons/I-balls*, *Phys. Rev. D* **D92** (2015) 105024 [[1508.01028](#)].
- [53] K. D. Lozanov and M. A. Amin, *Equation of State and Duration to Radiation Domination after Inflation*, *Phys. Rev. Lett.* **119** (2017) 061301 [[1608.01213](#)].
- [54] F. Hasegawa and J.-P. Hong, *Inflaton fragmentation in E-models of cosmological α -attractors*, *Phys. Rev. D* **D97** (2018) 083514 [[1710.07487](#)].
- [55] S. Antusch, F. Cefala, S. Krippendorf, F. Muia, S. Orani and F. Quevedo, *Oscillons from String Moduli*, *JHEP* **01** (2018) 083 [[1708.08922](#)].
- [56] J.-P. Hong, M. Kawasaki and M. Yamazaki, *Oscillons from Pure Natural Inflation*, *Phys. Rev. D* **D98** (2018) 043531 [[1711.10496](#)].
- [57] M. Ibe, M. Kawasaki, W. Nakano and E. Sonomoto, *Decay of I-ball/Oscillon in Classical Field Theory*, *JHEP* **04** (2019) 030 [[1901.06130](#)].
- [58] A. Arvanitaki, S. Dimopoulos, M. Galanis, L. Lehner, J. O. Thompson and K. Van Tilburg, *The Large-Misalignment Mechanism for the Formation of Compact Axion Structures: Signatures from the QCD Axion to Fuzzy Dark Matter*, [1909.11665](#).
- [59] S.-Y. Zhou, E. J. Copeland, R. Easther, H. Finkel, Z.-G. Mou and P. M. Saffin, *Gravitational Waves from Oscillon Preheating*, *JHEP* **10** (2013) 026 [[1304.6094](#)].
- [60] S. Antusch, F. Cefala and S. Orani, *Gravitational waves from oscillons after inflation*, *Phys. Rev. Lett.* **118** (2017) 011303 [[1607.01314](#)].
- [61] N. Kitajima, J. Soda and Y. Urakawa, *Gravitational wave forest from string axiverse*, *JCAP* **1810** (2018) 008 [[1807.07037](#)].
- [62] N. Kitajima and F. Takahashi, *Resonant conversions of QCD axions into hidden axions and suppressed isocurvature perturbations*, *JCAP* **1501** (2015) 032 [[1411.2011](#)].
- [63] R. Daido, N. Kitajima and F. Takahashi, *Domain Wall Formation from Level Crossing in the Axiverse*, *Phys. Rev. D* **D92** (2015) 063512 [[1505.07670](#)].
- [64] R. Daido, N. Kitajima and F. Takahashi, *Level crossing between the QCD axion and an axionlike particle*, *Phys. Rev. D* **D93** (2016) 075027 [[1510.06675](#)].
- [65] S.-Y. Ho, K. Saikawa and F. Takahashi, *Enhanced photon coupling of ALP dark matter adiabatically converted from the QCD axion*, *JCAP* **1810** (2018) 042 [[1806.09551](#)].
- [66] R. Daido, F. Takahashi and W. Yin, *The ALP miracle: unified inflaton and dark matter*, *JCAP* **1705** (2017) 044 [[1702.03284](#)].
- [67] F. Takahashi and W. Yin, *QCD axion on hilltop by a phase shift of π* , *JHEP* **10** (2019) 120 [[1908.06071](#)].
- [68] R. T. Co, E. Gonzalez and K. Harigaya, *Axion Misalignment Driven to the Hilltop*, *JHEP* **05** (2019) 163 [[1812.11192](#)].
- [69] G. R. Dvali, *Removing the cosmological bound on the axion scale*, [hep-ph/9505253](#).
- [70] T. Banks and M. Dine, *The Cosmology of string theoretic axions*, *Nucl. Phys. B* **B505** (1997) 445 [[hep-th/9608197](#)].
- [71] K. Choi, H. B. Kim and J. E. Kim, *Axion cosmology with a stronger QCD in the early universe*, *Nucl. Phys. B* **B490** (1997) 349 [[hep-ph/9606372](#)].
- [72] K. S. Jeong and F. Takahashi, *Suppressing Isocurvature Perturbations of QCD Axion Dark Matter*, *Phys. Lett. B* **B727** (2013) 448 [[1304.8131](#)].

- [73] R. Daido, F. Takahashi and W. Yin, *The ALP miracle revisited*, *JHEP* **02** (2018) 104 [[1710.11107](#)].
- [74] F. Takahashi and W. Yin, *ALP inflation and Big Bang on Earth*, *JHEP* **07** (2019) 095 [[1903.00462](#)].
- [75] I. G. Irastorza et al., *Towards a new generation axion helioscope*, *JCAP* **1106** (2011) 013 [[1103.5334](#)].
- [76] E. Armengaud et al., *Conceptual Design of the International Axion Observatory (IAXO)*, *JINST* **9** (2014) T05002 [[1401.3233](#)].
- [77] IAXO collaboration, E. Armengaud et al., *Physics potential of the International Axion Observatory (IAXO)*, *JCAP* **1906** (2019) 047 [[1904.09155](#)].
- [78] D. McKeen, *Cosmic neutrino background search experiments as decaying dark matter detectors*, *Phys. Rev.* **D100** (2019) 015028 [[1812.08178](#)].
- [79] Z. Chacko, P. Du and M. Geller, *Detecting a Secondary Cosmic Neutrino Background from Majoron Decays in Neutrino Capture Experiments*, *Phys. Rev.* **D100** (2019) 015050 [[1812.11154](#)].
- [80] PTOLEMY collaboration, M. G. Betti et al., *Neutrino physics with the PTOLEMY project: active neutrino properties and the light sterile case*, *JCAP* **1907** (2019) 047 [[1902.05508](#)].